

Microscopic calculation of symmetry projected nuclear level densities

K. Van Houcke,¹ S. M.A. Rombouts,¹ K. Heyde,¹ and Y. Alhassid²

¹*Universiteit Gent - UGent, Vakgroep Subatomaire en Stralingsfysica
Proeftuinstraat 86, B-9000 Gent, Belgium*

²*Center for Theoretical Physics, Sloane Physics Laboratory, Yale University
New Haven, Connecticut 06520, U.S.A.*

(Dated: September 27, 2018)

We present a quantum Monte Carlo method with exact projection on parity and angular momentum that is free of sign-problems for seniority-conserving nuclear interactions. This technique allows a microscopic calculation of angular momentum and parity projected nuclear level densities. We present results for the ⁵⁵Fe, ⁵⁶Fe and ⁵⁷Fe isotopes. Signatures of the pairing phase transition are observed in the angular momentum distribution of the nuclear level density.

PACS numbers: 21.10.Ma, 21.60.Ka, 21.60.Cs, 21.10.Hw

The level density is a fundamental property of a many-body system as all thermodynamical quantities can be derived from it. In nuclear physics, level densities are important because, according to Fermi's golden rule, they are critical for estimating nuclear reaction rates. The simplest approach to estimating the nuclear level density is to assume a free Fermi gas, leading to the well-known Bethe formula [1, 2]. A simple phenomenological way of incorporating pairing correlations and shell effects is to back-shift the excitation energy E_x by an amount Δ , resulting in the back-shifted Bethe formula.

The calculation of statistical nuclear reaction rates also requires knowledge of the angular momentum distribution of the nuclear level density. An empirical formula for the angular momentum distribution of the level density at a fixed excitation energy E_x assumes uncorrelated and randomly coupled single-particle spins, and is given by [3, 4]

$$\rho_J(E_x) = \rho(E_x) \frac{(2J+1)}{2\sqrt{2\pi}\sigma^3} e^{-\frac{J(J+1)}{2\sigma^2}}. \quad (1)$$

Here J is the angular momentum and σ is a spin-cutoff parameter, which can be used as an energy-dependent fitting parameter. The total level density $\rho(E_x)$ in (1) is often parametrized by a backshifted Bethe formula. The main drawback of this approach is that it requires a fit for each individual nucleus.

The microscopic calculation of the level density, and in particular its angular momentum distribution beyond the Fermi gas model and the spin-cutoff parametrization of Eq.(1) poses a complex problem. Recently, progress has been made both experimentally [5] and theoretically [6] in gaining more insight into the angular momentum distribution of level densities. The level density has been calculated microscopically using the shell model Monte Carlo (SMMC) method [7, 8]. Here, the effect of residual interactions between the nucleons is taken into account, although restricted to pairing plus multipole-multipole interactions that are free of the Monte Carlo sign problem. Angular momentum projection in the SMMC method was recently carried out for scalar observables by first projecting on the angular momentum component J_z [6]. Angular momentum projection introduces a new sign problem for $J \neq 0$ even when for a good-sign interaction. At

intermediate and high temperatures, this sign problem is sufficiently moderate to allow the reliable derivation of angular momentum distributions. However, at low temperatures this sign problem becomes more severe.

In this Letter, we present a new breakthrough that avoids sign problems at any value of angular momentum and/or particle number and that allows a microscopic test for the validity of the Fermi gas and spin-cutoff model for nuclei that exhibit strong pairing correlations. We discuss a quantum Monte Carlo (QMC) method to solve a general isovector $J = 0$ pairing model and solve the angular momentum projection problem for seniority conserving models. The pairing model serves as a benchmark to identify signatures of pairing correlations in the nuclear level density. In a finite nucleus, the number of paired particles is relatively small, and the identification of such signatures of the nuclear superfluid transition is difficult. Including higher order interaction multipoles, would also introduce a sign problem in our approach. Nonetheless, the projection is direct, and our QMC method allows us to treat the very large model spaces, which are needed for the calculation of level densities at higher excitation energies, and, particularly, for the study of the parity and angular momentum dependence of level densities (even at low excitation energy).

We start from a general isovector $J = 0$ pairing model, here written in the quasi-spin formalism [9, 10]

$$\hat{H} = \sum_j 2\varepsilon_j \hat{S}_j^0 - \sum_{jj'} g_{jj'} \hat{S}_j^+ \hat{S}_{j'}^-, \quad (2)$$

$$\hat{S}_j^0 = \frac{1}{2} \sum_{m>0} (\hat{a}_{jm}^\dagger \hat{a}_{jm} + \hat{a}_{j\bar{m}}^\dagger \hat{a}_{j\bar{m}} - 1),$$

$$\hat{S}_j^+ = \sum_{m>0} \hat{a}_{jm}^\dagger \hat{a}_{j\bar{m}}^\dagger, \quad \hat{S}_j^- = \sum_{m>0} \hat{a}_{j\bar{m}} \hat{a}_{jm}, \quad (3)$$

where the operator \hat{a}_{jm}^\dagger creates a particle in the spherical mean-field single-particle state $|jm\rangle$ with energy ε_j , and $|j\bar{m}\rangle$ is the time-reverse conjugate state of $|jm\rangle$. The operators $\hat{S}_j^0, \hat{S}_j^+, \hat{S}_j^-$ close an SU(2) algebra and are known as quasi-spin operators. The Hamiltonian (2) is exactly solvable for a constant pairing strength. The QMC method discussed here allows us to solve the general case when all terms in (2) are attractive, i.e., $g_{jj'} > 0$.

We formulate the pairing problem in the quasi-spin formalism to address the problem of the angular momentum projection. The quasi-spin projection S_j^0 determines the total number of particles $N_j = 2S_j^0 + \Omega_j$ in level j ($\Omega_j = j + 1/2$ is the pair degeneracy of orbital j), while the quasi-spin quantum number S_j determines the seniority quantum number $\nu_j = \Omega_j - 2S_j$, i.e., the number of unpaired particles in level j . Within this quasi-spin (or seniority) scheme, angular momentum remains a good quantum number. Given a set of quasi-spin quantum numbers S_j , one can determine the degeneracy for a given value of the total angular momentum J . Formally, the problem is equivalent to a chain of spins. The pairing interaction can flip spins such that the total ‘‘magnetization’’ $\sum_j S_j^0$ remains constant (particle number conservation). In addition, each quasi-spin quantum number S_j can take values between 0 and $\Omega_j/2$.

There exist a number of very efficient QMC approaches to simulate spin chains [11]. However, in our quasi-spin model, the value of $\sum_j S_j^0$ is fixed, while the quasi-spin values S_j can change. Recently, we developed a non-local loop update QMC scheme that is capable of sampling spin models at constant magnetization. In our case this means sampling the canonical ensemble [12]. Assuming the Hamiltonian $\hat{H} = \hat{H}_0 - \hat{V}$ consists of two non-commuting parts \hat{H}_0 and \hat{V} , our scheme is based on a perturbative expansion of the partition function at inverse temperature β

$$\text{Tr}(e^{-\beta\hat{H}}) = \sum_{m=0}^{\infty} \int_0^{\beta} d\tau_m \int_0^{\tau_m} d\tau_{m-1} \cdots \int_0^{\tau_2} d\tau_1 \text{Tr}[\hat{V}(\tau_1)\hat{V}(\tau_2)\cdots\hat{V}(\tau_m)e^{-\beta\hat{H}_0}], \quad (4)$$

with $\hat{V}(\tau) = \exp(-\tau\hat{H}_0)\hat{V}\exp(\tau\hat{H}_0)$. Here we choose

$$\hat{H}_0 = \sum_j 2\varepsilon_j \hat{S}_j^0 - \sum_j g_{jj} \hat{S}_j^+ \hat{S}_j^-; \quad \hat{V} = \sum_{j \neq j'} g_{jj'} \hat{S}_j^+ \hat{S}_{j'}^-. \quad (5)$$

The basic idea of the QMC method is to insert a so-called worm operator \hat{A} in the partition function, obtaining an extended partition function $\text{Tr}(\hat{A}e^{-\beta\hat{H}})$. By propagating this worm operator through imaginary time according to the rules explained in Ref. [12], one generates configurations that are distributed according to their weight in the canonical partition function $\text{Tr}_N(e^{-\beta\hat{H}})$ at fixed particle number N . Here, the worm operator is chosen to be $C + \sum_{ij} S_i^+ S_j^-$, with C a constant. Such a worm operator allows for the sampling of all configurations that correspond to a fixed set of quasi-spin quantum numbers S_j , without changing the value of $\sum_j S_j^0$. However, to be ergodic, the worm operator must also generate configurations with varying seniority quantum numbers, and therefore we add a worm operator that can change the values of the quasi-spins S_i , S_j and their projections S_i^0 , S_j^0 for two levels i and j such that $(S_i^0 + S_j^0)$ remains the same (particle-number conservation). The complete quasi-spin phase space is now sampled by propagating a seniority conserving worm operator and an additional seniority non-conserving worm operator. Additional details on the worm operator moves can be found in Ref. [12].

The moves of the worm operator can be constrained in such a way that the angular momentum J of the configuration does not change. Choosing the initial configuration with well defined angular momentum quantum number J enables us to calculate thermal averages for that fixed value of J . Parity is also a good quantum number in the quasi-spin basis, so that parity projection can be accomplished in a similar way.

We have used the QMC method outlined above to study the angular momentum and parity distribution of nuclear level densities in the presence of pairing correlations. We focused on the iron isotopes ^{55}Fe , ^{56}Fe and ^{57}Fe , within the complete $0f + 1p + 0g_{9/2}$ model space. To study truncation effects, we also consider an extended model space $1s + 0d + 0f + 1p + 0g_{9/2} + 2s + 1d$. The inverse temperature β ranges from 0 to 2.5 MeV^{-1} . For the mean-field potential, we used a Woods-Saxon potential with the parametrization of Ref. [13]. The single particle energies ε_j were obtained by diagonalizing this potential in a harmonic oscillator basis. For simplicity, we used a constant pairing strength (although our QMC method is not restricted to this case), determined to reproduce the experimental gap parameter $-1/2(\mathcal{B}(N-1, Z) - 2\mathcal{B}(N, Z) + \mathcal{B}(N+1, Z))$ for $Z = 26$ protons and $N = 30$ neutrons, with \mathcal{B} denoting the binding energy [2]. For the larger valence space, the value of pairing strength g is renormalized in such a way that the gap parameter remained fixed. Using the temperatures for which the heat capacity is maximal, we estimate our calculations to be free of truncation effects for excitation energies up to $E_x \lesssim 20 \text{ MeV}$ and $E_x \lesssim 50 \text{ MeV}$ for the $pf + g_{9/2}$ and $sd + pf + g_{9/2} + sd$ valence spaces, respectively. Total and angular momentum/parity-projected level densities are calculated as usual in the saddle point approximation.

Figure 1 shows the angular momentum distribution of the projected level density ρ_J at four different excitation energies E_x (we do not include not the magnetic degeneracy in ρ_J , i.e. $\rho(E_x) = \sum_J (2J+1)\rho_J(E_x)$). The solid squares are the QMC results (the statistical error are much smaller than the size of the squares), while the solid lines are the spin-cutoff model Eq. (1) fitted to the QMC data with σ^2 as a fit parameter. For all three iron isotopes, the angular momentum distribution becomes broader with increasing excitation energy. When this energy is sufficiently high ($E_x \geq 10 \text{ MeV}$), the QMC data are well described by the spin-cutoff model. For excitation energies $\leq 10 \text{ MeV}$, some deviations are observed. In particular, a staggering effect (in J) is found for the even-even ^{56}Fe isotope but not in the odd-even Fe isotopes. This effect was also reported in Ref. [6], where the interaction included higher multipoles, and was recognized as a signature of pairing correlations. Here, we observe a strong suppression of the $J = 1$ level density ($\rho_1 \approx \rho_0$), which is much smaller than the $J = 2$ level density. For higher angular momenta, we found only a very small staggering in the angular momentum dependence. This can be understood from the fact that the pairing interaction scatters only $J = 0$ nucleon pairs.

In a semiclassical approach, the spin-cutoff parameter is

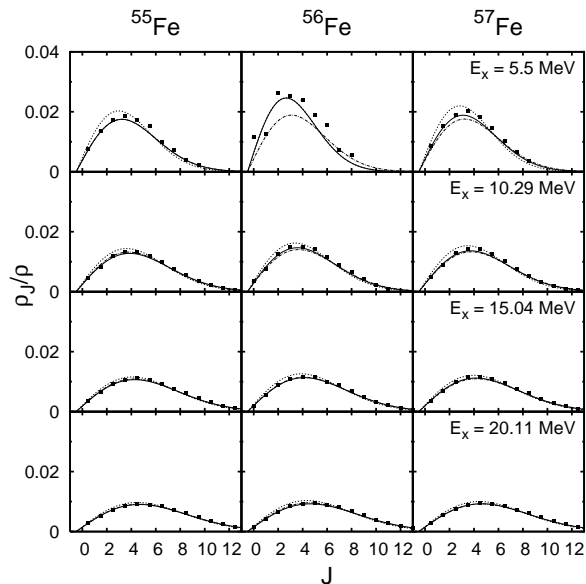


FIG. 1: The angular momentum distribution of the level density at a given excitation energy E_x for the iron isotopes ^{55}Fe , ^{56}Fe and ^{57}Fe . Solid squares are the Monte Carlo results in the $pf + g_{9/2}$ valence space. The solid lines are fits to the spin-cutoff model Eq. (1). Also shown are distributions given by the spin-cutoff model with σ^2 calculated from Eq. (7) using the rigid body moment of inertia (dotted-dashed lines), and from Eq. (6) (dotted lines).

given by

$$\sigma^2 = \frac{1}{3} \langle J^2 \rangle, \quad (6)$$

with $\langle \dots \rangle$ the thermal average at temperature T [14]. It is then common to define an effective moment of inertia from

$$I = \frac{\hbar^2}{T} \sigma^2. \quad (7)$$

The spin-cutoff parameter is often determined by substituting the rigid-body moment of inertia, $I = 2mA(r_0A^{1/3})^2/5$ in Eq. (7). (Here, r_0 is the nuclear radius parameter, A is the mass number and m is the nucleon mass). The spin-cutoff model (1) with σ^2 calculated from the rigid body moment of inertia (dotted-dashed lines in Fig. 1) essentially coincides for $E_x \geq 10$ MeV with the distribution fitted to the Monte Carlo data (solid lines in Fig. 1). For ^{56}Fe , however, for $E_x < 10$ MeV, the rigid-body moment of inertia predicts a broader angular momentum distribution than the one described by the fit. This indicates a reduction of the effective moment of inertia because of pairing correlations, and is a signature of nuclear superfluidity. We also determined σ^2 from the thermal average $\langle J^2 \rangle$, calculated directly in the QMC simulation. The angular momentum distributions using these spin-cutoff parameter are shown in Fig. 1 by the dotted lines. These distributions are slightly more peaked than the fitted distributions (solid lines), especially at low excitation energies ($E_x \leq 10$ MeV). For ^{56}Fe at $E_x = 5.5$ MeV, this curve coincides with the fit.

The top panels of Fig. 2 shows the effective moment of inertia as a function of excitation energy. At high excitation energy, the moment of inertia calculated from $\langle J^2 \rangle$ is very close to its rigid body value, the latter indicated with the horizontal dashed lines. We also calculated the spin-cutoff parameter σ^2 directly from the ratio $\rho_{0(1/2)}/\rho$ in the even (odd) case. The corresponding moments of inertia are also shown in the top panels of Fig. 2 (solid circles). These values seem to differ from our previous estimates of the moment of inertia, but they do not lead to significant differences in the angular momentum distributions, except for ^{56}Fe for $E_x < 10$ MeV. Here, the moment of inertia is strongly suppressed compared to ^{55}Fe and ^{57}Fe , due to $J = 0$ pairing.

The bottom panels of Fig. 2 show the pair correlation energy $\langle S^+ S^- \rangle = \langle \sum_{j,j'} S_j^+ S_{j'}^- \rangle$ as a function of excitation energy. It is seen that the pair correlation energy is strongly suppressed with increasing excitation energy. The suppressed neutron correlation energy of ^{55}Fe and ^{57}Fe is seen to increase first slightly with increased excitation energy (or temperature). This results from a blocking effect of the unpaired neutron at low temperatures.

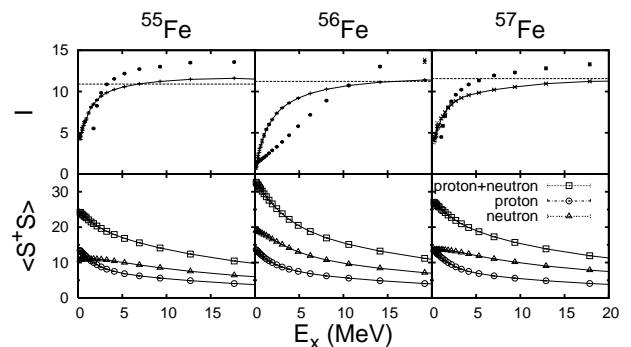


FIG. 2: Top panels: the moment of inertia I (in units \hbar^2) for ^{55}Fe (left), ^{56}Fe (middle) and ^{57}Fe (right). The horizontal dashed lines are the rigid body moments of inertia, the solid lines are moments of inertia calculated from Eq. (6), and the solid circles are from Eq. (7) with σ^2 determined via ρ_0/ρ (in the even-even case) and $\rho_{1/2}/\rho$ (in the odd-even case). Bottom panels: the pair correlation energy $\langle S^+ S^- \rangle$.

In Fig. 3 we show the parity-projected level density for $J = 0, 1, 2, 3$ as a function of excitation energy using the $sd + fpg + sd$ valence space. For energies below ~ 20 MeV, the angular momentum projected level densities show a strong parity dependence. Recently, angular momentum and parity-projected level densities were determined experimentally [5]. However, no parity dependence was resolved for level densities with specific values of J . Our calculations show that the angular momentum projected level density displays a strong parity dependence. For $J = 2$, we also show the level density within the smaller $pf + g_{9/2}$ valence space (dashed lines). Below ~ 20 MeV, the even-parity level density is in good agreement with the results found in the $sd + fpg + sd$ model space. However, the inclusion of the sd shells, below and above the

$pf + g_{9/2}$ shell, significantly enhances the odd-parity level density at low excitations. We found a similar effect for the total odd-parity level density. This results from the increased fraction of single-particle levels with positive parity.

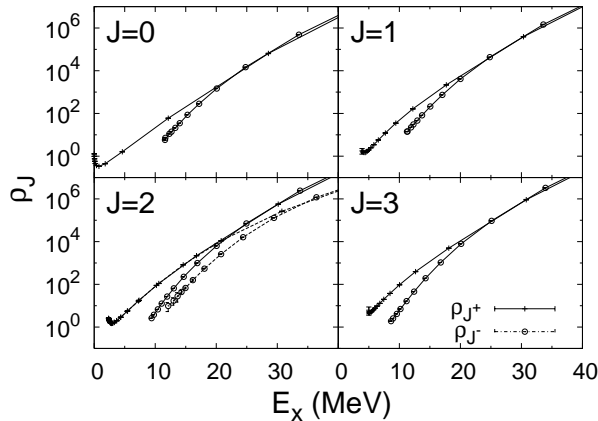


FIG. 3: The angular momentum and parity-projected level density of ^{56}Fe for the four lowest angular momentum values. A strong parity dependence is found for excitation energies up to ~ 20 MeV. The valence model space is $sd + pf + g_{9/2} + sd$. For $J = 2$, we also show results for the smaller $pf + g_{9/2}$ valence space (dashed lines).

In the left (right) panel of Fig. 4 we show the QMC total level density, as well as the angular momentum projected level densities $J = 0$ ($J = 1$) and $J = 2$ ($J = 3$) for ^{56}Fe . The QMC total level density is well described by the backshifted Bethe formula (fitted for $4.5 \text{ MeV} < E_x < 40 \text{ MeV}$) with Fermi gas parameter $a = 5.741 \pm 0.034 \text{ MeV}^{-1}$ and backshift $\Delta = 1.591 \pm 0.057 \text{ MeV}$ (see dotted-dashed line in Fig. 4). These are similar to the SMMC level density parameters $a = 5.780 \pm 0.055 \text{ MeV}^{-1}$ and $\Delta = 1.560 \pm 0.161 \text{ MeV}$ of Ref. [8], which were found to be in good agreement with the experimental level density. The present results indicate that the backshifted Bethe formula with temperature-independent parameter a works well up to higher energies [15]. The dashed lines of Fig. 4 are the angular momentum projected level densities, calculated from the total level density through Eq. (1) with rigid body σ^2 . At high excitation energy, these densities coincide with the QMC densities. However, for excitation energies below ~ 10 MeV, the QMC $J = 0$ level density deviates from the level density predicted by the spin-cutoff model with rigid body σ^2 . This is a signature of the pairing phase transition in the level density. This signature is also visible in the $J = 2$ level density for energies below ~ 8 MeV. For the odd J values, however, all QMC data are well described by the rigid body model.

In conclusion, we have used a quantum Monte Carlo method to calculate angular momentum and parity-projected level densities for a nuclear pairing model. This method allows us to calculate level densities in the very large model spaces that are necessary to avoid truncation effects. We have

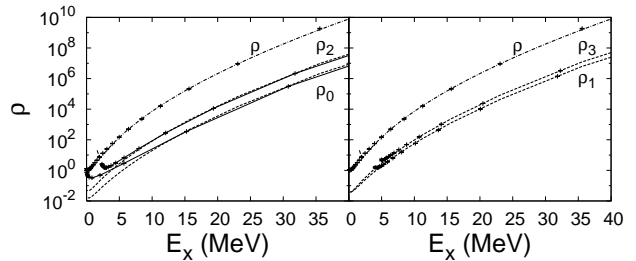


FIG. 4: The QMC total level density for ^{56}Fe , well described by the backshifted Bethe formula (dotted-dashed line), together with the projected densities $J = 0$, $J = 2$ (left panel), and $J = 1$, $J = 3$ (right panel). The solid lines connect the J -projected Monte Carlo results, while the dashed lines show the projected level density from the spin-cutoff model Eq. (1) using the rigid body values of σ^2 .

found that pairing correlations affect the angular momentum distribution of the level density at low excitation energies, thereby revealing signatures of the pairing phase transition in nuclei.

We thank N. Jachowicz and K. Langanke for interesting suggestions and discussions. We acknowledge the financial support of the Fund for Scientific Research - Flanders (Belgium) and IUAP, and of the U.S. DOE grant No. DE-FG-0291-ER-40608.

-
- [1] H.A. Bethe, Phys. Rev. **50**, 332 (1936); Rev. Mod. Phys. **9**, 69 (1937).
 - [2] A. Bohr and B.R. Mottelson, *Nuclear Structure. Volume I: Single Particle Motion*, Benjamin, New York, (1969).
 - [3] C. Bloch, Phys. Rev. **93**, 1094 (1954).
 - [4] T. Ericson, Adv. Phys. **9**, 425 (1960).
 - [5] Y. Kalmykov *et al.*, Phys. Rev. Lett. **96**, 012502 (2006).
 - [6] Y. Alhassid, S. Liu and H. Nakada, nucl-th/0607062.
 - [7] S.E. Koonin, D.J. Dean and K. Langanke, Phys. Rep. **278**, 1 (1997). ; W.E. Ormand, Phys. Rev. C **56**, R1678 (1997); S. Rombouts, K. Heyde and N. Jachowicz, Phys. Rev. C **58**, 3295 (1998); K. Langanke, Phys. Lett. B **438**, 235 (1998); Y. Alhassid, G. F. Bertsch, S. Liu and H. Nakada, Phys. Rev. Lett. **84**, 4313 (2000).
 - [8] H. Nakada and Y. Alhassid, Phys. Rev. Lett. **79**, 2939 (1997).
 - [9] D.J. Dean and M. Hjorth-Jensen, Rev. Mod. Phys. **75**, 607 (2003).
 - [10] D.M. Brink and R.A. Broglia, *Nuclear Superfluidity*, Cambridge University Press, Cambridge (2005).
 - [11] N. Kawashima and K. Harada, J. Phys. Soc. Jpn. **73**, 1379 (2004).
 - [12] S. Rombouts, K. Van Houcke and L. Pollet, Phys. Rev. Lett. **96**, 180603 (2006); K. Van Houcke, S. Rombouts and L. Pollet, Phys. Rev. E **73**, 056703 (2006).
 - [13] C. M. Perey and F. G. Perey, Nucl. Data Tables **10**, 540 (1972).
 - [14] Y. Alhassid *et al.*, Phys. Rev. C **72**, 064326 (2005).
 - [15] Y. Alhassid *et al.*, Phys. Rev. C **68**, 044322 (2003).